Korean J. Chem. Eng., **31**(9), 1539-1546 (2014)
DOI: 10.1007/s11814-014-0067-6

pISSN: 0256-1115
eISSN: 1975-7220

Experimental study on performance of steam-water injector with central water nozzle arrangement

Wen Jun Li, Dao Tong Chong†, Jun Jie Yan, Wei Xiong Chen, and Jin Shi Wang

State Key Laboratory of Multiphase Flow in Power Engineering, Xi'an Jiaotong University, Xi'an 710049, China
(*Received 9 September 2013 • accepted 24 February 2014*)

Abstract−The steam-water injector (SI) is a simple mechanical device that has been widely used in industry. We did an experimental study to find the influence of physical and geometrical parameters on performance of the SI. The physical parameters studied were steam inlet pressure, water inlet pressure and water inlet temperature. Whereas, the geometrical parameters studied were steam nozzle area ratio, area ratio of steam nozzle to water nozzle and the mixing section converging angle. Pump head was introduced to evaluate the lifting-pressure performance of the SI under different operating and geometrical conditions. Optimal values of steam nozzle area ratio and mixing section converging angle were 1.3 and 11.6° respectively, for the present work, and optimal value of area ratio of steam nozzle to water nozzle increased with increasing water inlet pressure. Two head-capacity curves were introduced to highlight the effect of various physical and geometrical parameters on the performance of SI.

Keywords: Steam-water Injector, Parametric Analysis, Entrainment Ratio, Pump Head, Head-capacity Characteristic

INTRODUCTION

The steam injector (SI) is a simple, compact and passive device without moving parts, in which steam is used as the energy source to pressurize water [1]. The SI consists of four main parts: steam nozzle, water nozzle, mixing chamber and diffuser, and no moving parts are needed. As a result, the SI has been applied in many industries, such as district-heating system [2], refrigeration [3,4], petroleum engineering [5], and desalination system [6,7]. Especially in nuclear reactors, the SI used for emergency core cooling and feedwater supply has been developed by many researchers [8-11].

According to the positions of steam nozzle and water nozzle, the SI can be classified into two categories: SI with central steam nozzle arrangement and SI with central water nozzle arrangement. These two types of SI have attracted much study to of their working mechanism and performance. Cattadori et al. [9] carried out a test on the one-stage high-pressure SI with central steam nozzle arrangement to study the influence of inlet steam pressure and inlet water temperature on the performance of the SI. However, the influence of geometrical parameters was not included. Deberne and Leone [1] used a simple global model to predict the performance of the steam injector with central water nozzle arrangement, and the influence of three parameters (one geometrical parameter, the mixing section outlet diameter and two physical parameters, the inlet steam pressure and inlet water temperature) was studied. Beithou and Aybar [12,13] developed a mathematical model for the SI and discussed the influence of physical parameters (inlet steam pressure, inlet water pressure and temperature) on system performance. Effects of water volumetric flow rate, chamber height and geometrical parameters of an ejector on gas suction rate and gas phase holdup were studied by Kim et al. [14]. SI with central steam nozzle arrangement was studied experimentally by Yan et al. [2,15] to report the effect of some geometrical and physical parameters on the lifting-pressure performance. Steam ejector used in refrigeration cycle was experimentally studied by Ruangtrakoon et al. [16] to investigate the influence of steam nozzle geometries on the system performance. The influence of steam nozzle geometries on flow structure of a SI was studied numerically in 2D domain by Dai and Huo [17]. Shah et al. [18,19] studied the SI with central steam nozzle arrangement experimentally and computationally to report the characteristics of the SI and effect of mixing section length on direct-contact condensation.

In recent studies, the exergy analysis was used as a tool to evaluate exergy losses in the SI. Trela et al. [20-22] studied exergy losses in individual parts of the SI, and an indirect method was used to determine exergy losses in the two-phase region. According to the exergy of inlet steam, inlet water and discharged water, exergy efficiency was calculated by Yan et al. [23] and Cai et al. [24] in an effort to improve performance of the SI.

To the best knowledge of the authors, previous studies mainly focused on the applications of the SI and development of mathematical models. The influence of physical parameters on the performance of the SI has been reported; however, the influence of geometrical parameters has seldom been mentioned, especially for the SI with central water nozzle arrangement. In the present work, an experiment of the SI with central water nozzle arrangement was carried out to find out the influence of physical parameters (inlet steam pressure, inlet water pressure and temperature) and geometrical parameters (steam nozzle area ratio, mixing chamber angel and area ratio of steam nozzle to water nozzle) on its performance. Moreover, pump head-capacity characteristic of the SI was discussed. These experimental results would be helpful in design and

†To whom correspondence should be addressed.
E-mail: dtchong@mail.xjtu.edu.cn

economic operation of the SI.

EXPERIMENTAL APPARATUS

The experimental system, shown in Fig. 1, mainly consists of an electric steam generator, a SI, three water tanks, five water pumps and a cooling tower. The SI is the core of the experimental system and a schematic diagram of the SI with central water nozzle arrangement is shown in Fig. 2. It mainly consists of a water nozzle, a converging-diverging steam nozzle, a mixing chamber, and a diffuser. The steam nozzle is an annular gap between the exterior of water nozzle and the interior of mixing chamber. During the experiment, steam and water exchange heat, momentum (due to temperature and velocity difference) and mass (due to condensation of steam) in the mixing chamber. The steam-water two-phase flow transforms into supersonic flow, and a condensation shock wave appears in the mixing chamber, where steam condenses into water at relatively high pressure. After the shock wave, the pressurized and heated water flows into water tank 3. If valve 2 is opened, the heated water would flow into the cooling tower to maintain the inlet water temperature. Otherwise the heated water would flow into water tank 2, which increases the inlet water temperature.

The temperatures are measured by K-type thermocouples. The

Table 1. Test conditions in present experiment

Parameters	Values
Inlet water pressure, $p_{0,w}$ [MPa]	0.2-0.8
Inlet water temperature, $t_{0,w}$ [°C]	20-60
Inlet steam pressure, $p_{0,s}$ [MPa]	0.15-0.40
Steam nozzle throat area, A_{cr} [mm^2]	160-388
Steam nozzle outlet area, $A_{1,sn}$ [mm^2]	224-577
Water nozzle outlet diameter, $d_{1,wn}$ [mm]	8
Mixing chamber throat diameter, d_{th} [mm]	8
mixing section converging angle, δ [°]	8.3-16.7

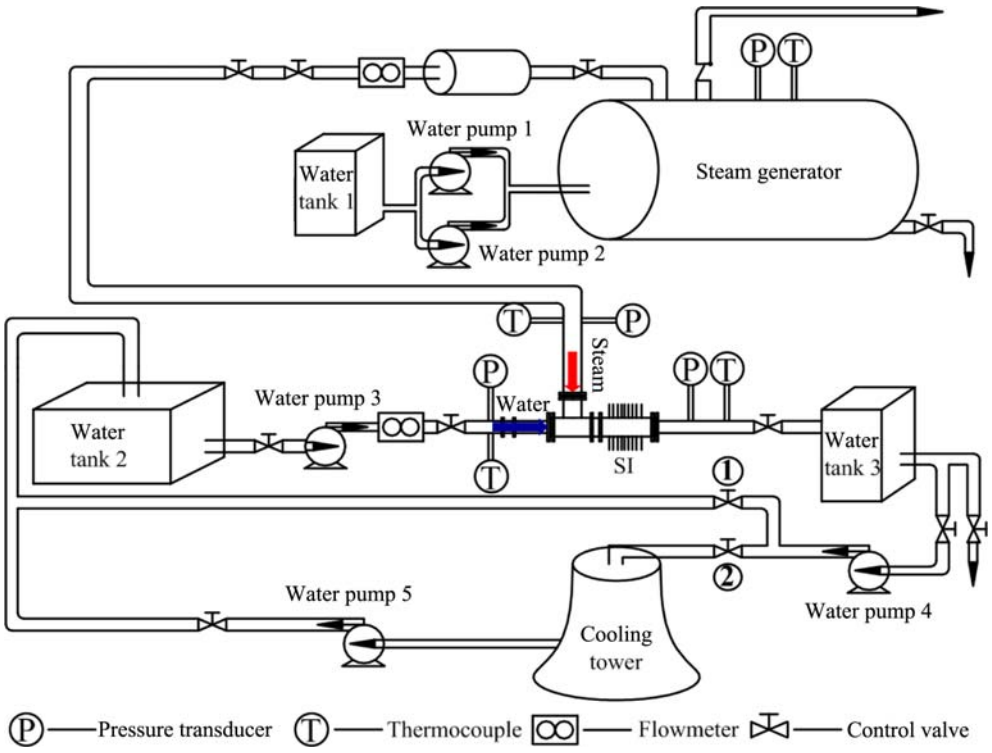

Fig. 1. A schematic diagram of experimental system.

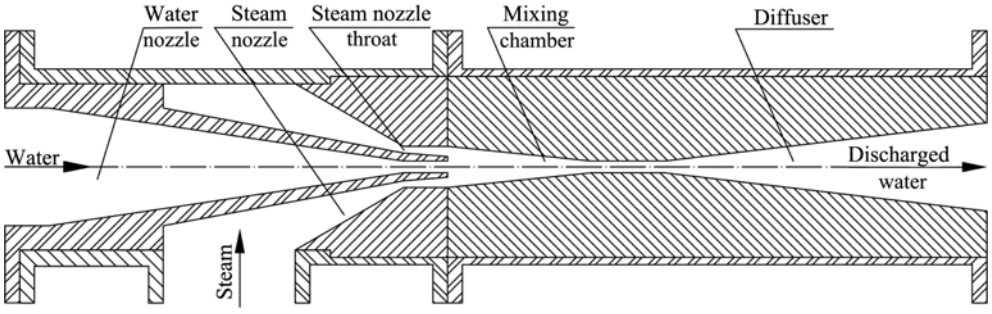

Fig. 2. A schematic diagram of SI with central water nozzle arrangement.

thermocouples are calibrated by a standard thermometer with an accuracy of 1 K. The pressures are all measured by MSI pressure transducers, with the accuracy of 0.2% FS. The inlet water volumetric flow rate is measured by the electrical flowmeter, with the accuracy of 0.5% FS. The inlet steam mass flow rate is measured by Coriolis mass flowmeter, with the accuracy of 0.2% FS. Details of test conditions are given in Table 1.

RESULTS AND DISCUSSIONS

The steady-state operation characteristics of the SI have been studied in terms of three independent physical parameters:

- Inlet steam pressure, $p_{0,s}$
- Inlet water pressure, $p_{0,w}$
- Inlet water temperature, $t_{0,w}$

The function of steam nozzle and water nozzle is to accelerate steam and water, resulting in high speed flow [18,19]. Velocity at steam nozzle and water nozzle exit has great influence on velocity of steam-water two-phase flow in the mixing section, and void fraction in the mixing section mainly depends on mass flow rate at steam nozzle and water nozzle exit. So, performance of the SI is greatly affected by steam nozzle and water nozzle exit conditions. To reflect these factors, three independent geometrical parameters were introduced:

- Steam nozzle area ratio

$$f_{sn}=\frac{A_{1,sn}}{A_{cr}} \tag{1}$$

- Area ratio of steam nozzle to water nozzle

$$f_{sn,wn}=\frac{A_{cr}}{A_{1,wn}} \tag{2}$$

- Mixing section converging angle, δ

where A_{cr} is the area of steam nozzle throat, $A_{1,sn}$ is the area of steam nozzle exit plane, $A_{1,wn}$ is the area of water nozzle exit plane. With increasing the steam nozzle area ratio, Mach number at steam nozzle exit plane increases and pressure at steam nozzle exit plane decreases, provided inlet steam pressure is kept constant [25].

The main dependent parameters are:

- Inlet steam mass flow rate, m_s
- Inlet water mass flow rate, m_w
- Discharge water pressure, p_d
- Discharge water mass flow rate, m_d

1. Entrained Steam Mass Flow Rate

Steam through the converging-diverging steam nozzle can be generally accelerated to supersonic speed due to the vacuum mainly produced by the severe steam condensation, and then the steam mass flow rate can be calculated as [26].

$$m_s=A_{cr}\sqrt{2\frac{\kappa}{\kappa+1}\left(\frac{2}{\kappa+1}\right)^{\frac{2}{\kappa-1}}\frac{p_{0,s}}{v_{0,s}}} \tag{3}$$

Calculated and measured steam mass flow rate variation with inlet steam and water pressure is shown in Fig. 3. It can be observed that the steam mass flow rate is almost kept constant with increasing the inlet water pressure, provided the inlet steam pressure is kept constant. On the other hand, the steam mass flow rate increases with increasing the inlet steam pressure. Moreover, the measured values are in good agreement with calculated values, which indicates that the assembly accuracy of the SI can be ensured.

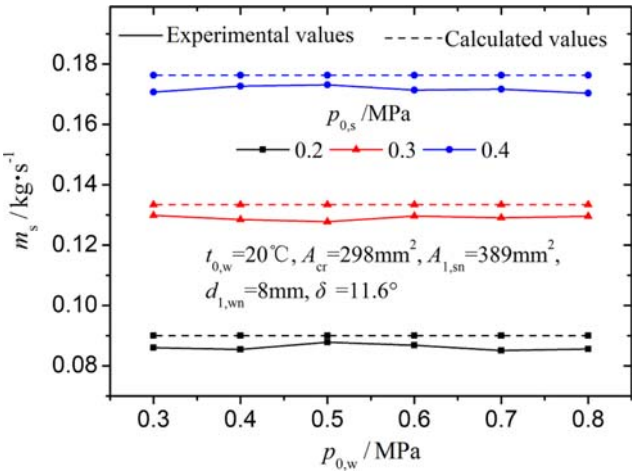

Fig. 3. Entrained steam mass flow rate.

2. Influence of Physical Parameters on Performance of the SI

2-1. Entrainment Ratio

Entrainment ratio represents the mass of steam entrained by unit mass of water, expressed as:

$$\phi=\frac{m_s}{m_w} \tag{4}$$

With increasing the inlet water pressure, inlet water mass flow rate increases and inlet steam mass flow rate is kept constant as shown in Fig. 3. With increasing the inlet steam pressure, back pressure of water nozzle increases [2,15], which decreases inlet water flow rate. Meanwhile, inlet steam mass flow rate increases with steam inlet pressure as shown in Fig. 3. So, entrainment ratio increases with increasing the inlet steam pressure but decreases with increasing the inlet water pressure as shown in Fig. 4. With increasing the inlet water temperature, back pressure of water nozzle increases [2,15],

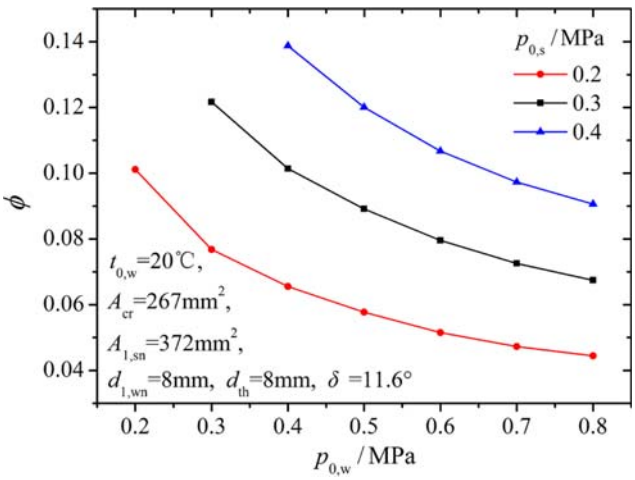

Fig. 4. Entrainment ratio under various inlet steam and water pressures.

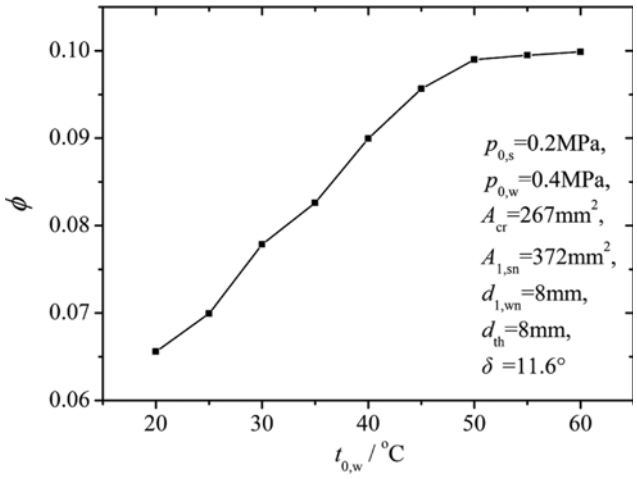

Fig. 5. Entrainment ratio under various inlet water temperatures.

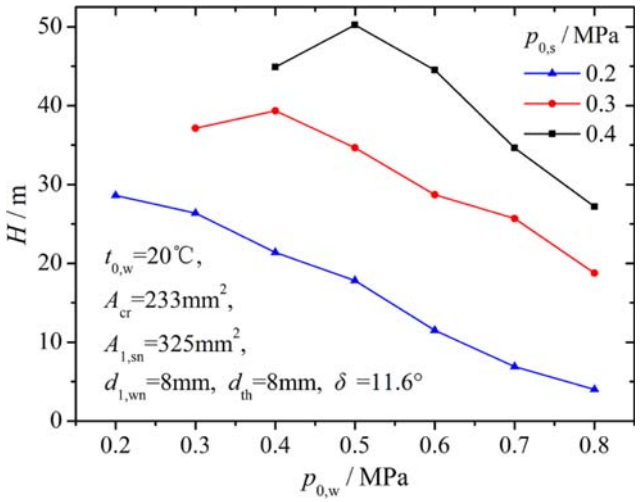

Fig. 6. Pump head under various inlet steam and water pressures.

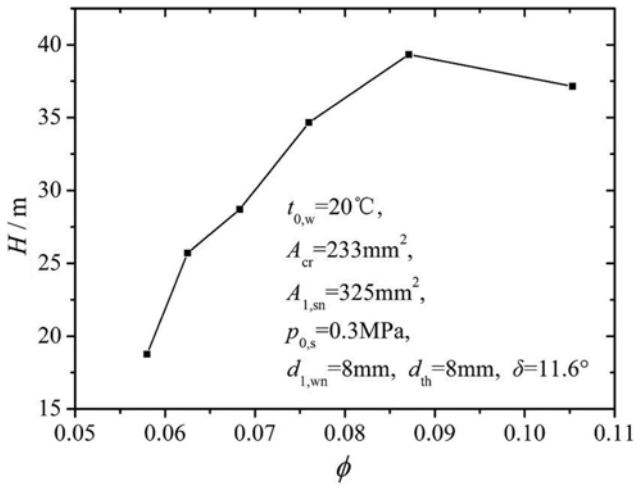

Fig. 7. Pump head under various entrainment ratios.

which decreases inlet water flow rate. Meanwhile inlet steam mass flow rate is kept constant. So, entrainment ratio increases with increasing the inlet water temperature as shown in Fig. 5. However, temperature difference between steam and water decreases with increasing the inlet water temperature, which weakens the heat, mass and momentum transfer between steam and water and decreases the increasing rate of water nozzle back pressure. So under high inlet water temperature, entrainment ratio increases very slightly with increasing the inlet water temperature.

2-2. Pump Head

The SI has a self-adaptive characteristic, which has been reported by Yan et al. [15]. Less than the maximum discharge pressure, the SI can self-adjust the discharge pressure to the operation requirements, while the inlet steam and water parameters and mass flow rate are kept constant. Moreover, its application in industry mainly depends on its maximum discharge pressure. So, it is necessary to investigate the lifting-pressure performance of the SI.

The SI can pressurize the water by the energy source of steam. It can be treated as a kind of pump and the pump head is introduced to evaluate the lifting-pressure performance of the SI in the present work. It represents the increase in mechanical energy of water in the SI, expressed as:

$$H = \frac{p_d - p_{0,w}}{\rho_w g} \tag{5}$$

Steam is used to pressurize cold water in the SI [1]. Due to the collision between steam and water in mixing chamber, momentum of steam is partly transferred to that of water. That means the increase in mechanical energy of cold water comes from the kinetic energy of steam. With increasing the inlet steam pressure, steam mass flow rate and velocity at steam nozzle exit increase, which causes an increase in input kinetic energy of the mixing chamber. Moreover, the increase in velocity at steam nozzle exit enhances moment transfer in mixing chamber. So pump head increases with increasing the inlet steam pressure in the present work as shown in Fig. 6.

Entrainment ratio represents the mass ratio of steam to water, so it has a great influence on void fraction in mixing chamber. An appropriate void fraction in the mixing chamber can lead to a lower sound velocity and a higher Mach number of steam-water two-phase flow. In this case, pressure after the shock increases and lifting-pressure performance of the SI is strengthened. Pump head increases first, then decreases with increasing the entrainment ratio as shown in Fig. 7. With increasing the inlet water pressure, entrainment ratio decreases. Therefore, pump head increases first then decreases with increasing the inlet water pressure. However, no peak has been found in the present work when inlet steam pressure is low (0.2 MPa) as shown in Fig. 6. When inlet steam pressure is low, entrainment ratio is low even though inlet water pressure is low. With increasing the inlet water pressure, entrainment ratio becomes lower. So under low inlet steam pressure (0.2 MPa), pump head decreases with increasing the inlet water pressure as shown in Fig. 6.

Pump head decreases with increasing the inlet water temperature as shown in Fig. 8. Steam is used as the energy source to pressurize water in the SI [1]. However, with increasing the inlet water temperature, temperature difference between steam and water decreases which weakens heat, mass and momentum transfer between steam and water. On the other hand, the entrainment ratio increases quickly with increasing in inlet water temperature as shown in Fig. 5, which leads to the steep increase in void fraction and sound velocity in

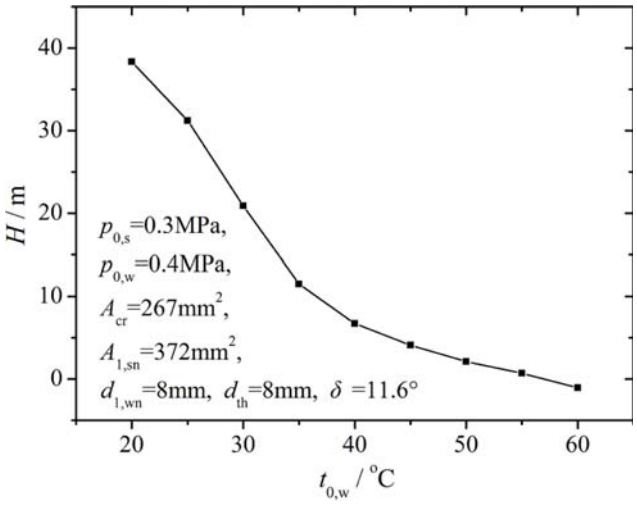

Fig. 8. Pump head under various inlet water temperatures.

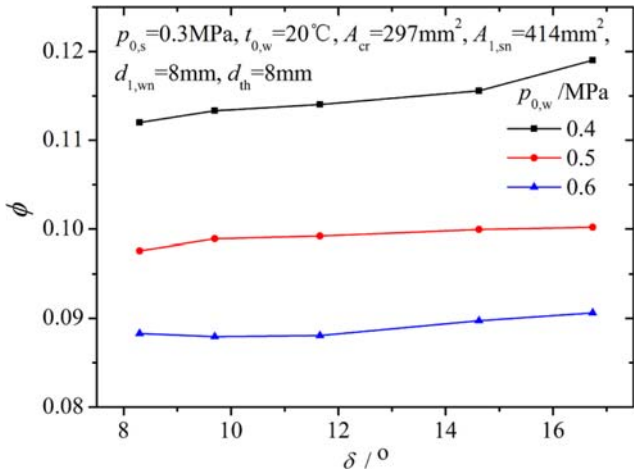

Fig. 10. Entrainment ratio under various mixing section converging angles.

the mixing chamber. Moreover, with increasing the inlet water temperature, pressure of steam-water two-phase flow in the mixing section increases which leads to the decrease in velocity in the mixing section [2]. Thus lifting-pressure performance of the SI is weakened with increasing the inlet water temperature.

3. Influence of Geometrical Parameters on Performance of the SI

3-1. Entrainment Ratio

With increasing the steam nozzle area ratio, steam nozzle outlet pressure decreases. Then the back pressure of water nozzle decreases, which leads to the increase in inlet water mass flow rate. Entrainment ratio decreases slightly with increasing the steam nozzle area ratio as shown in Fig. 9.

As a converging channel, the mixing chamber is immediately adjacent to the steam nozzle exit. The supersonic steam turns suddenly through an angle due to the mixing chamber. The result is a straight oblique shock wave, aligned at an angle relative to the oncoming flow and it causes a sudden increase in pressure [27]. With increasing the mixing section converging angle, intensity of the oblique shock wave increases, which leads to the increase in back pressure of water nozzle. Entrainment ratio increases slightly with increasing the mixing section converging angle as shown in Fig. 10.

In the present work, the area of water nozzle exit is kept constant, and area ratio of steam nozzle to water nozzle is changed by changing the area of steam nozzle throat. With increasing the area of steam nozzle throat, inlet steam water mass flow rate and area ratio of steam nozzle to water nozzle increase. Thus entrainment ratio increases obviously with increasing the area ratio of steam nozzle to water nozzle as shown in Fig. 11.

3-2. Pump Head

Pump head increases first then decreases with increasing the steam nozzle area ratio as shown in Fig. 12. Steam nozzle area ratio does not particularly influence entrainment ratio as shown in Fig. 9, but the condition of steam at steam nozzle exit is greatly affected by it. Provided the other parameters are kept constant, the velocity and Mach number at steam nozzle exit increase with increasing the nozzle area ratio. Thus the mass, momentum and heat transfer between steam and cold water is enhanced, which increases the velocity and Mach number of steam-water two-phase flow in the mixing chamber.

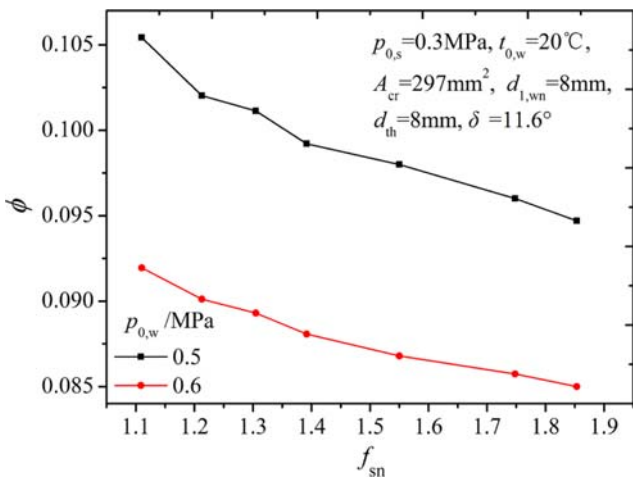

Fig. 9. Entrainment ratio under various area ratios of steam nozzle.

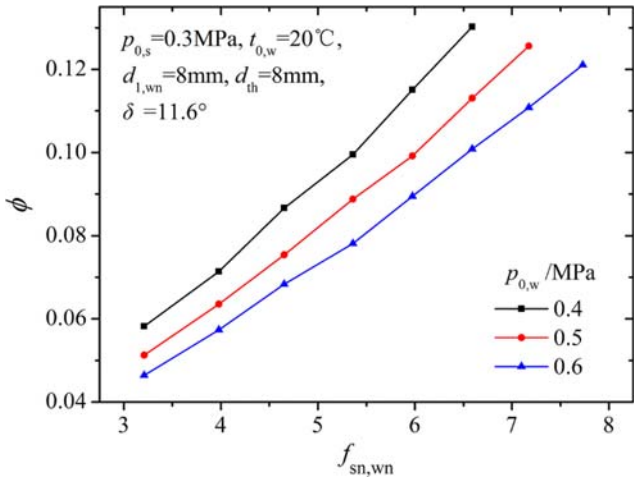

Fig. 11. Entrainment ratio under various area ratios between steam nozzle and water nozzle.

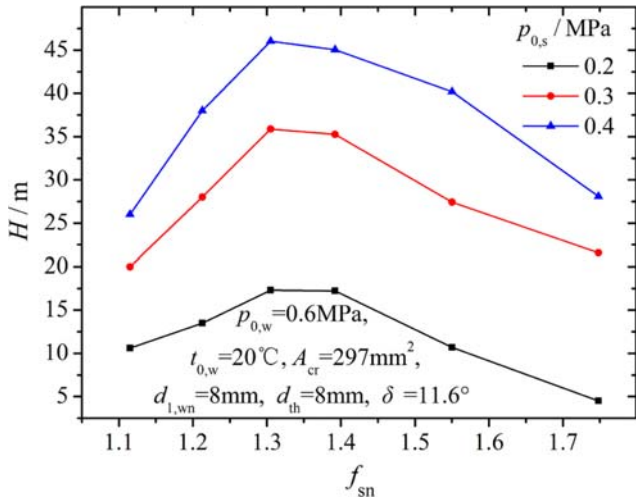

Fig. 12. Pump head under various area ratios of steam nozzle.

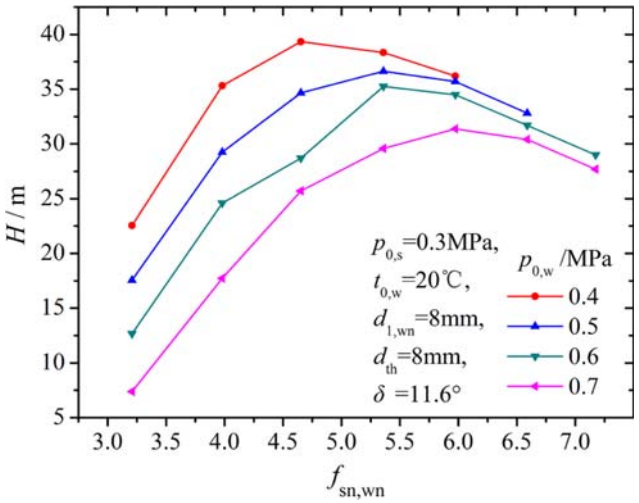

Fig. 14. Pump head under various area ratios between steam nozzle and water nozzle.

In this case, pressure after the shock increases and lifting-pressure performance of the SI is strengthened. But if the nozzle area ratio is too big, a normal shock wave develops at a section between the throat and the exit plane of the steam nozzle, which causes a sudden drop in velocity to sub-sonic levels [27]. In this case, the velocity and Mach number of steam-water two-phase flow decrease and lifting-pressure performance of the SI is weakened. Therefore, an appropriate steam nozzle area ratio can ensure high lifting-pressure performance. The optimal value of steam nozzle area ratio is 1.3 for the present work.

The effect of mixing section converging angle on pump head is shown in Fig. 13. When the mixing section converging angle is large, which means that the length of mixing section is short and the steam-water two-phase flow is not uniformly mixed. With decreasing the mixing section converging angle, the steam and water could be mixed more uniformly. But if the angle is too small, the length of the converging channel becomes too long. In this case, steam has almost condensed completely in the mixing chamber and void fraction in the throat of mixing chamber becomes too small, which weakens the intensity of condensation shock wave. On the other hand, the intensity of oblique shock wave at steam nozzle exit (as explained in section 3.3.1) increases with increasing the mixing section converging angle. With increasing the intensity of the oblique shock wave, velocity and Mach number of steam decreases, which weakens the mass, momentum and heat transfer between steam and water. In this case, lifting-performance of the SI is weakened. Therefore, there should be an appropriate mixing section converging angle, which could result in an optimal pump head of the SI. The optimal value of mixing section converging angle is 11.6° for the present work.

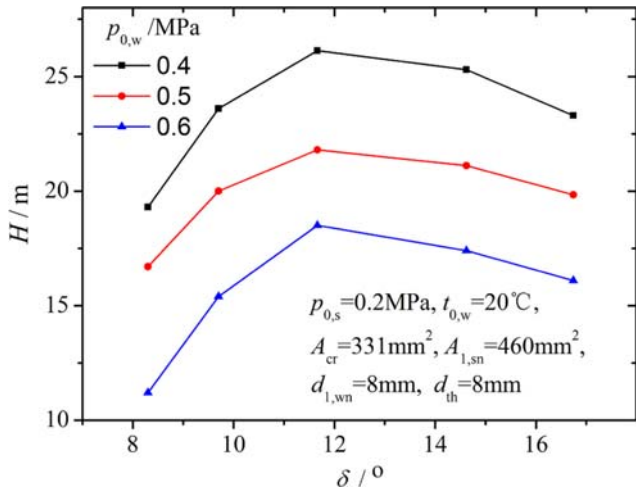

Fig. 13. Pump head under various mixing section converging angles.

When the inlet physical parameters are kept constant, entrainment ratio mainly depends on the area of steam nozzle throat and water nozzle exit. An appropriate area ratio of steam to water nozzle can ensure an optimal entrainment ratio, which strengthens lifting-pressure performance of the SI. Therefore, an optimal area ratio of steam nozzle to water nozzle can be found to ensure an optimal lifting-pressure performance as shown in Fig. 14. Moreover, optimal value of area ratio of steam nozzle to water nozzle increases with increasing the inlet water pressure, in the range of 4.65-5.97. That is because water mass flow rate increases with increasing the inlet water pressure. Steam mass flow rate should increase to match the increase in water mass flow rate. Therefore, under given inlet steam pressure, area of steam nozzle throat increases in order to increase the steam mass flow rate.

4. Head-capacity Curves for SI

When the flow rate of a pump varies, the head changes too. Plotting the head against the flow rate, head-capacity characteristic of pump can be obtained. In the present work, head-capacity curve was introduced to describe the character of the SI.

Two head-capacity curves have been obtained in the present work as shown in Figs. 15 and 16. Under low inlet steam pressure (0.2 MPa, Fig. 15), pump head decreases with increasing the discharge water mass flow rate. While under high inlet steam pressure, pump head increases first, then decreases with increasing the discharged water mass flow rate, called drooping head-capacity curve [28]. The reason is similar to that for Fig. 6 as mentioned in section 3.2.2. Moreover, the drooping characteristic of traditional pumps (such as centrif-

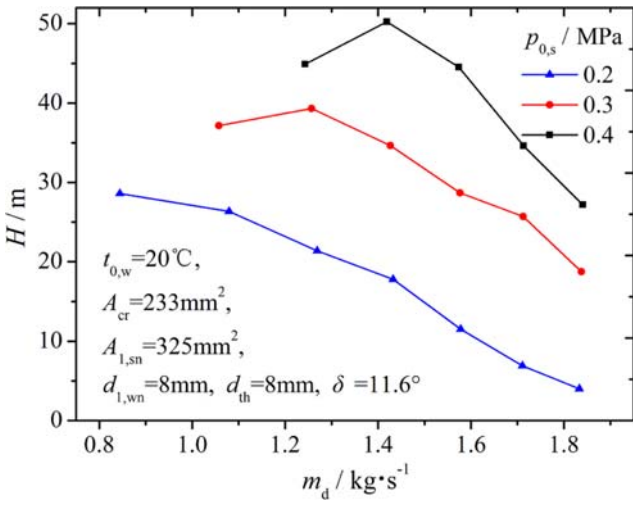

Fig. 15. Head-capacity characteristic under various inlet steam pressures.

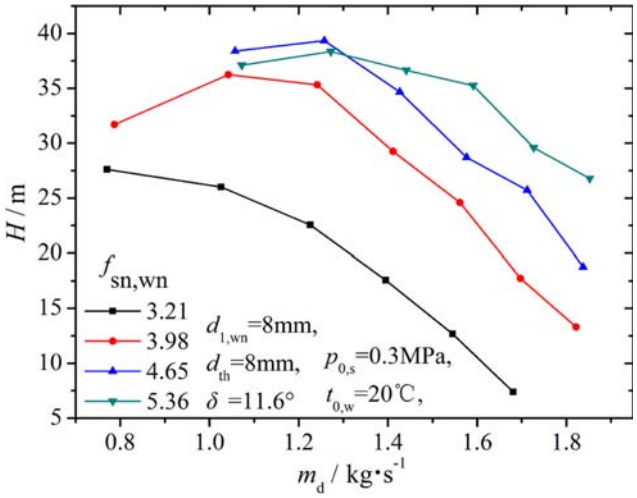

Fig. 16. Head-capacity characteristic under area ratios between steam nozzle and water nozzle.

ugal pump) may lead to unstable operation in certain systems [28]. But the SI can overcome this shortcoming. As mentioned above, the SI can self-adjust the discharge pressure to the operation requirements in certain range, meanwhile discharge water mass flow rate is kept constant, provided inlet physical parameters are kept constant [5]. So, the drooping characteristic of head-capacity curve cannot affect the stable operation of the SI.

With increasing the discharge water mass flow rate, the entrainment ratio decreases. An appropriate entrainment ratio can ensure a high pump head as shown in Fig. 7. Pump head increases first, then decreases with increasing the discharge water mass flow rate as shown in Fig. 16. However, no peak has been found in the present work for low (3.21) area ratio of steam nozzle to water nozzle as shown in Fig. 16. When this area ratio is low (3.21), entrainment ratio is low even though water mass flow rate is low. In this case, the lifting-pressure process is deteriorated. With increasing the water mass flow rate, the entrainment ratio becomes lower. Pump head thus decreases monotonically with increasing the discharge water flow rate. Moreover, the higher the area ratio of steam nozzle to water nozzle, the flatter the head-capacity curves.

Both steam nozzle area ratio and mixing section converging angle do not particularly influence the entrainment ratio as shown in Figs. 9 and 10. With changing these two parameters, the shape of head-capacity curves does not change in the present work.

CONCLUSIONS

The performance of the SI with central water nozzle arrangement was studied experimentally under various parameters of steam, water, steam nozzle, water nozzle and mixing chamber. The main results are as follows:

(1) Influence of physical parameters on performance of the SI was discussed. Entrainment ratio increases with increasing the inlet steam pressure and inlet water temperature, but decreases with increasing the inlet water pressure. Pump head increases with increasing the inlet steam pressure in the present test conditions. It decreases sharply with increasing the inlet water temperature. It increases first then decreases with increasing the inlet water pressure. So it is very valuable to operate the SI under low water temperature.

(2) Influence of geometrical parameters on performance of the SI was presented. Steam nozzle area ratio and mixing section converging angle has little influence on entrainment ratio, but it increases obviously with increasing the area ratio of steam nozzle to water nozzle. Pump head increases first and then decreases with increasing the steam nozzle area ratio. Similar trends were found for mixing section converging angle and area ratio of steam nozzle to water nozzle.

(3) For the present work, optimal values of inlet water pressure increase with increasing the inlet steam pressure. Optimal values of steam nozzle area ratio and mixing section converging angle were 1.3 and 11.6° respectively, and the optimal value of area ratio of steam nozzle to water nozzle increased with increasing water inlet pressure, in the range of 4.65-5.97. These experimental results would be helpful in design of the SI.

(4) Two shapes of head-capacity curves were obtained. Drooping head-capacity curves were obtained for high inlet steam pressure and area ratio of steam nozzle to water nozzle. The drooping characteristic cannot affect the stable operation due to self-adaptive characteristic of the SI. Under both low inlet steam pressure and low area ratio of steam nozzle to water nozzle, degressive head-capacity curves were obtained. The higher the area ratio of steam nozzle to water nozzle, the flatter the head-capacity curves.

ACKNOWLEDGEMENTS

This project has been supported by National 973 Program of China (No. 2009CB219803) and National Natural Science Foundation of China (No. 51006081, No. 51125027).

NOMENCLATURE

A : area [m^2]
d : diameter [mm]
f : area ratio
g : gravity acceleration [m/s^2]

H : pump head [m]
m : mass flow rate [kg/s]
p : pressure [MPa]
t : temperature [°C]
v : specific volume [m^3/kg]

Greek Symbols

δ : mixing section converging angle, °
κ : specific heat ratio
ρ : density [kg/m^3]
Φ : entrainment ratio

Subscripts

0 : inlet
1 : outlet
cr : throat of steam nozzle
d : discharged water
th : throat of mixing chamber
sn : steam nozzle
w : water
wn : water nozzle

REFERENCES

1 N. Deberne, J. F. Leone, A. Duque and A. Lallemand, *Int. J. Multiphase Flow*, **25**, 841 (1999).
2. J. J. Yan, S. F. Shao, J. P. Liu and Z. Zhang, *Appl. Therm. Eng*., **25**, 1153 (2005).
3. Y. Bartosiewicz, Z. Aidoun and Y. Mercadier, *Appl. Therm. Eng*., **26**, 604 (2006).
4. P. Srisastra and S. Aphornratana, *Appl. Therm. Eng*., **25**, 2247 (2005).
5. I. Fujita, M. Yoshie and K. Takezaki, *Oceans 2007 Europe International Conference*, Aberdeen, Scotland, 1221 (2007).
6. R. S. Kumar, A. Mani and S. Kumaraswamy, *Desalination*, **179**, 345 (2005).
7. R. S. Kumar, S. Kumaraswamy and A. Mani, *Desalination*, **204**, 437 (2007).
8. S. K. Malibashev, *At. Energ*., **79**, 498 (1995).
9. G. Cattadori, L. Galbiati, L. Mazzocchi and P. Vanini, *Int. J. Multiphase Flow*, **21**,591 (1995).
10. T. Narabayashi, W. Mizumachi and M. Michitugu, *Nucl. Eng. Des*., **175**, 147 (1997).
11. T. Narabayashi, W. Mizumachi, M. Michitugu and S. Ohmori, *Nucl. Eng. Des*., **200**, 261 (2000).
12. N. Beithou and H. S. Aybar, *J. Eng. Gas Turb. Power*, **123**, 693 (2001).
13. N. Beithou and H. S. Aybar, *J. Eng. Gas Turb. Power*, **123**, 701 (2001).
14. O. S. Kim, Y. Lee and D. H. Lee, *Korean J. Chem. Eng*., **26**, 288 (2009).
15. J. J. Yan, X. Z. Wu, D. T. Chong and J. P. Liu, *Heat Transfer Eng*., **32**, 88 (2011).
16. N. Ruangtrakoon, S. Aphornratana and T. Sriveerakul, *Exp. Therm. Fluid Sci*., **35**, 676 (2011).
17. X. C. Dai and J. Huo, *Appl. Mech. Mater*., **130**, 1703 (2012).
18. A. Shah, I. R. Chughtai and M. H. Inayat, *Int. J. Multiphase Flow*, **37**, 1305 (2011).
19. A. Shah, I. R. Chughtai and M. H. Inayat, *Int. J. Heat Mass Tran*., **58**, 62 (2013).
20. M. Trela, R. Kwidzinski, D. Butrymowicz and J. Karwacki, *Appl. Therm. Eng*., **30**, 340 (2010).
21. M. Trela and R. Kwidzinski, *Arch. Thermody*., **29**, 41 (2008).
22. M. Trela, R. Kwidzinski and D. Butrymowicz, *Chem. Process Eng*., **29**, 455 (2008).
23. J. J. Yan, D. T. Chong and X. Z. Wu, *Appl. Therm. Eng*., **30,** 623 (2010).
24. Q. Cai, M. W. Tong and X. J. Bai, *Korean J. Chem. Eng*., **29**, 513 (2012).
25. B. R. Munson, D. F. Young and T. H. Okiishi, *Fundamentals of fluid mechanics*, Inc., Wiley (2005).
26. D. L. Zeng, L. J. Zhao and Y. Xiao, *Proceedings of the International Conference on Energy Conversion and Application*, Wuhan, China, **1**, 65 (2001).
27. Y. A. Cengel and M. A. Boles, *Thermodynamics - an engineering approach*, McGraw Hill (2006).
28. M. Volk, *Pump characteristics and applications*, CRC Press, Taylor and Francis Group (2005).